

Identification of Operational Regions in the Chemical-Looping with Oxygen Uncoupling (CLOU) Process with a Cu-based Oxygen Carrier

Iñaki Adánez-Rubio, Alberto Abad*, Pilar Gayán, Luis F. de Diego, Francisco García-Labiano, Juan Adánez

Instituto de Carboquímica (ICB-CSIC), Dept. of Energy & Environment, Miguel Luesma Castán, 4, Zaragoza, 50018, Spain

*Corresponding author. Tel.: +34 976 733977; fax: +34 976 733318

Email address: abad@icb.csic.es

Con formato: Inglés (Estados Unidos)

Abstract

Chemical-Looping with Oxygen Uncoupling (CLOU) is an alternative chemical-looping process for the combustion of solid fuels with inherent CO₂ capture. The CLOU process demands a material as oxygen carrier with the ability to decompose with O₂ release at suitable temperatures for solid fuel combustion, e.g. copper oxide. This article presents an experimental method to determine the maximum oxygen generation rate of an oxygen carrier as well as to determine the minimum solid inventory that must be used in the fuel reactor. The method here proposed can be used as basis for comparison of the use of different oxygen carriers or type of coals. In this work, the combustion of coal by using a promising Cu-based oxygen carrier prepared by the spray drying method was tested. The oxygen carrier (Cu60MgAl) was composed of 60 wt.% CuO and MgAl₂O₄ was used as supporting material. Experiments were carried out in a batch fluidized-bed reactor at temperatures ranging from 900 to 980 °C. Three different regions were identified depending on the oxygen carrier to coal mass ratio. For oxygen carrier to coal ratios higher than 50 (Region I), coal was fully converted to CO₂ and H₂O. In addition, an excess of oxygen was present in the flue gases, which was close to the equilibrium concentration. When this ratio was in the range 50-25 (Region II), the concentration of oxygen was decreasing whereas some CO was observed as the only unconverted gas. Further decrease in the oxygen carrier to coal ratio below 25 (Region III) caused the depletion of oxygen in the exhaust gases but CO remained as the only

unconverted gas. CH₄ or H₂ were never detected at the reactor outlet in any case and agglomeration problems were never observed. These regions were related to the solids inventory in the fuel reactor by the rate of oxygen generation calculated in every case. A maximum rate of oxygen generation for the oxygen carrier was determined as kg O₂/s per kg of oxygen carrier, which increased with the temperature from $2.1 \cdot 10^{-3}$ at 930 °C to $2.8 \cdot 10^{-3}$ at 980 °C. From these values, the estimated solids inventory in the fuel reactor was changed from 39 at 930 °C to 29 kg/MW_{th} at 980 °C. The results obtained in this work showed that in the CLOU process it is possible to reach full conversion of the solid fuel with very low solids inventory and avoiding the oxygen polishing step.

Keywords: Carbon capture, combustion, coal, CLOU, copper

1. Introduction

According to the IPCC report on mitigation of climate change [1], which considers different possible growing scenarios, Carbon Capture and Storage (CCS) would contribute with 15–55% to the cumulative mitigation effort worldwide until 2100 in order to stabilize CO₂ concentration in the atmosphere. CCS is a process involving the separation of CO₂ emitted by industry and energy-related sources, and its storage for isolation from the atmosphere over a long term. Chemical-Looping Combustion process (CLC) has been suggested among the best alternatives to reduce the economic cost of CO₂ capture using fuel gas [2] and to increase the efficiency with respect to other CO₂ capture process [3]. In this process, CO₂ is inherently separated from other combustion products, N₂ and unused O₂, through the use of a solid oxygen carrier and thus no energy is expended for the separation. The CLC process has been demonstrated for gaseous fuel combustion such as natural gas and syngas in 10 to 140 kW_{th} units using oxygen carrier materials based on Ni [4,5], Cu [6] and Fe [7,8]. A review of the materials developed to be used as oxygen carrier is found in Adánez et al. [9].

Solid fuels are considerably more abundant and less expensive than natural gas. Thus, the use of the CLC concept for coal combustion can be highly relevant. First option to use solid fuels in a CLC process was to use syngas in the fuel reactor coming from a previous gasifying step. However, it is necessary to use pure oxygen for gasification of the solid fuel to apply this technology. This step has an important energy penalty due to the oxygen separation from the

air. The second option of development is the Chemical-Looping Combustion with coal, where the solid fuel is directly introduced to the fuel reactor. Even other kinds of solid fuels could be used, e.g. biomass or solid wastes [10]. Here, the solid fuel is physically mixed with the oxygen carrier in the fuel reactor, which is fed with a gaseous stream of a gasifying agent, e.g. steam or CO₂. Thus, volatiles and the gas products from coal gasification are converted to CO₂ and H₂O by reaction with the oxygen carrier particles in the fuel reactor. The limitation in the solid fuel conversion in the CLC with coal comes from the slow gasification process [10-12]. To increase the gasification rate, temperatures higher than 1000 °C have been proposed to be used in the fuel reactor [12].

An alternative process, Chemical-Looping with Oxygen Uncoupling (CLOU), was recently proposed by Mattisson and coworkers [13] making use of the idea first proposed by Lewis and Gilliland [14] to produce CO₂ from solid carbonaceous fuels by using gaseous oxygen produced by the decomposition of CuO. The CLOU process is based on the strategy of using oxygen carrier materials which release gaseous oxygen in the fuel reactor and thereby allowing the solid fuel to burn with gas phase oxygen. These materials can be also regenerated at high temperatures. In this way, the slow gasification step on the CLC process with solid fuels is not necessary, giving a much faster fuel conversion [15,16]. In CLOU process, fluidization gas can be recycled CO₂. In this process, the use of steam is not necessary, contrary to the case of CLC with coal [11].

Leion et al. [17] using six different solid fuels show that the differences in reactivity between fuels were more pronounced in CLC with solid fuels using steam as gasification agent than in CLOU process. This fact was explained by the difference in the reaction paths between CLC and CLOU processes. In CLC the limiting reaction is the slow coal gasification, which is strongly affected by the temperature and coal type. However, they stated that the rate of oxygen release from the oxygen carrier particles becomes the limiting step in the CLOU process. Thus, the type of fuel used has lower relevance in the conversion rate. Experiments carried out at 980 °C using petroleum coke as fuel [15] showed that CLOU process can increase the fuel conversion by a factor of 45 with respect to the conversion found when the same fuel was gasified with steam and using Fe-based oxygen carriers which do not release oxygen in the fuel reactor. A quantification of the role of oxygen uncoupling in accelerating the gasification of solid fuels was also confirmed by Eyring et al. [18] and Abad et al. [16] using Cu-based oxygen carrier materials.

Con formato: Inglés (Estados Unidos)

Con formato: Inglés (Estados Unidos)

Fig. 1 shows a schematic diagram of a CLOU system. In the fuel reactor the fuel conversion is produced by different reactions. First the oxygen carrier releases oxygen according to:



and the solid fuel begins devolatilization producing a carbonaceous solid (char, mainly composed by carbon and ash) and volatile matter as gas product :



Then, char and volatiles are burnt as in usual combustion with gaseous oxygen according to reactions (3) and (4):



After steam condensation, a pure CO₂ stream can be obtained. The reduced oxygen carrier is transported to the air reactor, where the oxygen carrier is regenerated to the initial oxidation stage with the oxygen of the air, and being ready for a new cycle. Ideally, the exit stream of the air reactor contains only N₂ and unreacted O₂. The heat release over the fuel and air reactors is the same as for conventional combustion. Therefore, CO₂ is inherently captured in the CLOU process, and a low energy penalty for CO₂ separation and low CO₂ capture costs are expected as in the CLC process.

About the oxygen carrier, only those metal oxides that have a suitable equilibrium partial pressure of oxygen at temperatures of interest for combustion (800-1200 °C) can be used as CLOU oxygen carriers for solid fuel combustion. Besides, this O₂ release must be reversible in order to oxidize the oxygen carrier in the air reactor and regenerate the material. Thus a special requirement is needed for the oxygen carrier to be used in the CLOU process in comparison to oxygen carriers for normal CLC, where the fuel must be able to react directly with the oxygen carrier without any release of gas phase oxygen. CuO/Cu₂O, Mn₂O₃/Mn₃O₄, and Co₃O₄/CoO have been identified as redox pairs with capacity to evolve oxygen at high temperature [13].

The temperature in the air and fuel reactors in the CLOU process must be adjusted according to the thermodynamic equilibrium and reaction kinetics in order to optimize the process [18]. Thus, the operating conditions for the air reactor are constrained due to the thermodynamics

of the oxidation of the oxygen carrier. As example, Fig. 2 shows the partial pressure of oxygen as a function of the temperature for the CuO/Cu₂O system, calculated using HSC software [19]. The oxygen concentration at equilibrium conditions greatly depends on the temperature. Thus, the equilibrium concentration at 900 °C is 1.5 vol.% O₂ for CuO/Cu₂O system, whereas it increases up to 12.4 vol.% at 1000 °C. Therefore, if the acceptable oxygen concentration from the air reactor was maximum 4.5 vol.%, Cu₂O should be oxidized to CuO below 950 °C. Higher temperature in the air reactor would cause a higher fraction of unused oxygen.

Moreover, the equilibrium concentration of oxygen in the fuel reactor will be given by the temperature in the reactor; which is determined by the temperature of the incoming particles, the circulation rate, as well as the heat of reaction in the fuel reactor. For example, the overall reaction with C is exothermic in the fuel reactor for copper oxide, as it is showed in reaction (5). Thus it is possible to have a temperature increase in the fuel reactor, which results in a significantly higher partial pressure of O₂ at equilibrium conditions.



A high equilibrium partial pressure of oxygen together with a very reactive oxygen carrier will promote the overall conversion rate of the solid fuel in the fuel reactor. In addition, the combustion of the fuel will decrease the oxygen concentration in the reactor and can improve the decomposition reaction of the metal oxide particles. However, it should be desirable to get low concentration of oxygen from the fuel reactor in order to obtain a high purity CO₂ stream. Similar conclusions can be inferred from thermodynamics of other materials.

There are only a small number of materials proposed in the literature dealing with the use of Cu- [16-18,20,21], and Mn-based [22-26] based materials for CLOU process. An overview of the characteristics of these materials can be found in [9, 20,21].

In the research group at Chalmers University of Technology, 20 different CLOU materials were tested in batch fluidized bed for combustion of gaseous (CH₄) or solid fuels [13, 15, 17, 22-23, 25]. Good results were obtained using an oxygen carrier based on CuO and ZrO₂ as support [13,17]. Although there were some defluidization phenomena during some parts of the experiments, no permanent agglomerations were detected. Cyclic testing with solid fuels in the temperature range of 880-985 °C verified a very rapid release of oxygen and combustion of fuel started with a high conversion rate. Regarding the use of manganese

oxides for CLOU process, Shulman et al. [22] analyzed the CLOU properties of different Mn-based materials combined with Fe_2O_3 , NiO or SiO_2 prepared by freeze granulation. They found that some Mn/Fe oxygen carriers showed very high reactivity towards methane. Further, other Mn/Fe materials prepared by spray drying were tested by the same research group [23]. One of them was successfully applied for the combustion of methane in a continuously operated unit [24]. The authors apply this quality to open the possibility to combine benefits of CLOU and CLC processes in the future for the combustion of gaseous fuels. A manganese ore was also tested for CLOU by Rydén et al. [24] in a continuous unit using CH_4 , but this material was much less reactive than synthetic Mn/Fe particles. Other material with a spinel perovskite-like type structure, $\text{CaMn}_{0.875}\text{Ti}_{0.125}\text{O}_3$, [25, 26] was also evaluated as an oxygen carrier for CLOU process. Conversion rates were lower than those found for Cu-based CLOU materials, although it was still higher compared to normal CLC with solid fuels.

In the research group of ICB-CSIC [20,21], a screening study was carried out considering more than 25 different Cu-based oxygen carriers prepared by different methods, using several supporting materials and varying the copper content. The reaction rates for oxygen release and oxygen carrier regeneration were determined carrying out successive cycles in a TGA system at different reaction temperatures and oxygen concentrations. Selected materials were tested by redox decomposition-regeneration cycles in a batch fluidized-bed reactor working at different temperatures and reacting atmospheres. The fluidization behaviour against agglomeration and attrition during a high number of cycles was determined. Two promising Cu-based oxygen carriers prepared by pelletizing by pressure (60 wt.% CuO supported on MgAl_2O_4 , and 40 wt.% CuO supported on ZrO_2) were selected for further studies using coal as fuel. These materials exhibited high reactivity during successive redox cycles. In addition, a low attrition rate was measured and agglomeration was never detected.

After the screening tests, it was decided to prepare a Cu-based material (60 wt.%) supported on MgAl_2O_4 by the industrial preparation method spray drying (Cu60MgAl). Similar particles to those previously prepared by pelletization by pressure were obtained. So, new spray dried particles were tested in a continuously operated CLOU unit using coal as fuel [16]. In this work it was demonstrated the proof of the concept of CLOU process for coal combustion using a Cu-based oxygen carrier. The fuel reactor temperature was varied from 900 °C to 960 °C and the solids inventory was decreased from 1150 to 235 kg/MW_{th}. In all experiments

complete combustion to CO₂ and H₂O of fuel and high carbon capture efficiency was measured. The carbon capture efficiency depended on the fuel reactor temperature ranging from 97 % at 900 °C to 99.3 % at 960 °C. These findings suggested that good performance in coal combustion could be obtained even if the solids inventory was lower than 235 kg/MW_{th}. However, further decrease of the solids inventory was not possible due to operational limitations of CLOU unit.

The aim of this work was to investigate the performance of the Cu60MgAl material as oxygen carrier for the CLOU process. The minimum solids inventory to get full combustion of coal was determined by a new method applied to CLOU process. The rate of oxygen release was determined when batches of “El Cerrejon” coal particles were added to a fluidized-bed reactor containing the oxygen carrier material. Different oxygen carrier to fuel ratios were used, as well as several temperatures between 900 and 950 °C were tested. The minimum solids inventory in the fuel reactor was inferred from the maximum rate of oxygen release obtained at every temperature

1. Experimental

1.1. Cu-based oxygen carrier

The oxygen carrier used was a Cu-based material prepared by spray drying. Oxygen carrier particles were manufactured by VITO (Flemish Institute for Technological Research, Belgium) using MgAl₂O₄ spinel from Baikowski, grade S30CR and CuO from PRS PANREAC (96% CuO) as raw materials. The CuO content was 60 wt.%. After particles were formed by spray drying the particles were calcined for 12 h at 1100 °C and sieved (100-300 μm). Particles were calcined for a second time to increase the mechanical strength. Thus, oxygen carrier particles had a total calcination time of 24 h at 1100 °C. These particles are referred to as Cu60MgAl.

Oxygen carrier particles were physically and chemically characterized by different techniques. Main characteristics are shown in Table 1. The mechanical strength, determined using a Shimpo FGN-5X crushing strength apparatus, was taken as the average value of the force needed to fracture a particle obtained in 20 measurements. Identification of crystalline

chemical species was carried out by powder X-ray diffractometer Bruker AXS graphite monochromator.

The mechanical strength of the particles after 24 h of calcination was adequate for its use in a fluidized bed. The compounds found by XRD analysis were CuO and $MgAl_2O_4$. The oxygen transport capability, R_{OC} , was calculated as $R_{OC} = (m_{ox} - m_{red})/m_{ox}$, m_{ox} being the mass of completely oxidized particles and m_{red} the mass in the reduced form, i.e. when all CuO has been reduced to Cu_2O .

1.2. Fuel

The fuels used were a bituminous Colombian coal “El Cerrejón” and char prepared with this coal. This is the same fuel used in previous work in a continuous CLOU unit [16]. The coal particle size used in this study was +200-300 μm . This coal showed a high swelling behaviour, which could promote agglomeration of the fluidized bed. In order to avoid coal swelling, the coal was subjected to a thermal pre-treatment for pre-oxidation. Coal was heated at 180 °C in air atmosphere for 28 hours [27]. Elemental and proximate analyses of the fresh and pre-treated coal are shown in Table 2. The pre-oxidation causes an increase in the oxygen content from 7 to 17.6 %.

The char was produced by devolatilization of pre-treated bituminous Colombian coal “El Cerrejón”. To produce the char, a batch of 500 g of coal particles was devolatilized in a fluidized-bed reactor. The reactor was fluidized by N_2 and it was heated up from room temperature to 900°C with a temperature ramp of 20°C/min and afterwards cooled down. Since the gas velocity increases with the temperature, the N_2 flow was correspondingly reduced as the temperature increased to ensure bubbling bed conditions and to avoid elutriation of particles. The proximate and ultimate analysis of the obtained char is also shown in Table 2. The particle size of char was in the range +200-300 μm , and the density of the particles was about 1000 kg/m^3 .

1.3. Experimental setup: batch fluidized-bed reactor

Reduction-oxidation multi-cycles were carried out in a fluidized-bed reactor to know the oxygen release behaviour of the oxygen carrier in similar operating conditions to that existing in the CLOU process. The experimental work was carried out in a setup consisting of a fluidized-bed reactor, a system for gas feeding, a solid fuel feeding system, and the gas

analysis system. A schematic layout of the laboratory setup is presented in Fig. 3. The reactor –55 mm inner diameter and 700 mm height– is electrically heated by a furnace, and had a preheating zone just under the distributor plate.

The reactor was loaded with 240 g of solid material. Solids are placed above the distributor plate, ensuring a bed height about 50 mm at static conditions. In order to have good fluidizing behaviour, a particle size fraction of +100-200 μm was used in the bed. The minimum fluidizing velocity was $4 \cdot 10^{-3}$ m/s for the smallest particle size and $1.5 \cdot 10^{-3}$ m/s for the biggest one. The terminal velocity was 0.33 m/s and 1.15 m/s, respectively. In some test, the oxygen carrier was diluted in alumina particles (+200-400 μm). In these test the total mass of solids was 240g, but it was possible to operate with lower amount of oxygen carrier.

The temperature inside the bed was measured and used to control the reaction temperature. The reactor had pressure taps in order to measure the absolute pressure in the bed and the pressure drop. Agglomeration and defluidization problems could be detected by a sharp decrease in the bed pressure drop during operation. The pressure tap was also useful to detect possible blocking in the downstream pipes due to possible elutriated particles or tar condensation in cold points.

The gas feeding system had different mass flow controllers connected to an automatic three-way valve. In this way, it was possible to feed alternatively air or nitrogen. The total fluidizing flow was 200 $\text{L}_\text{N}/\text{h}$, which corresponds to a gas velocity of 0.1 m/s at 900 °C in the reactor. Different gas analyzers measured continuously the gas composition at the reactor exit after water condensation. CO, CO₂ and CH₄ dry basis concentrations were determined using non-dispersive infrared analysis (NDIR) and H₂ by thermal gas conductivity. The O₂ concentration was determined in a paramagnetic analyzer.

The feeding system of the solid fuel consisted of a fuel chute which ends 20 mm above the distributor plate and about 50-60 mm below the upper level of the fluidizing particles. So, solid fuel particles are fed inside the fluidized bed. The upper part of the chute has a valve system that creates a reservoir in which the fuel is placed. Coal particles were fed by valve v1 to a small reservoir placed in the upper part of the fuel chute, see Fig. 3. After that, the deposit was over-pressurized 1 bar with N₂ by valve v2. Once the reservoir was pressurized, valve v2 was closed and v3 was opened and quickly closed. Then, coal particles fall down to the fluidized bed through the fuel chute as the reservoir is unpressurized. Thus, it was ensured

that coal particles were forced to enter to the fluidized bed, whereas a continuous flow of nitrogen through the fuel chute is avoided.

The oxygen carrier particles were exposed sequentially to reducing and oxidizing conditions. During reduction periods, batches of “El Cerrejón” coal were fed to the reactor through the solids feeding system whereas the reactor was fluidized with N_2 . Every load was left till coal combustion was complete or the oxygen carrier was fully reduced, which usually happened in less than 120 s. After every reducing period, oxygen carrier particles were fully re-oxidized with air before starting a new cycle.

1.4. Experimental planning

The experimental work was carried out at temperatures between 900 and 950 °C, which is the intended temperature interval in the fuel reactor in a CLOU process with Cu-based materials [16]. The temperature of the reactor was fixed before starting the reducing or oxidizing period, but during reaction the temperature could increase up to 50 °C because the exothermic reaction when coal is burnt or the Cu_2O was oxidized.

Three series of experiments were performed to increase the oxygen carrier to coal ratio in the range covered. The first tests were done with an amount of 240 g of oxygen carrier material in the bed. This batch of particles was exposed to a total number of 35 reduction/oxidation cycles, corresponding to 31 hours of hot fluidization in order to evaluate possible variations in the oxygen carrier reactivity during redox cycles or the appearance of operational problems during fluidization using coal as fuel. The temperature was fixed to 925 °C at the starting of the reduction period. In this case, the loads of coal between 0.2 and 2 g were added. Thus, very high oxygen carrier to coal mass ratios were used (in the range 1200-120), but the fluidization behaviour of the oxygen carrier could be analyzed without interference of using a diluting material.

The second and third series were carried out with the oxygen carrier diluted in alumina particles. Thus, the mass fraction of the oxygen carrier in the bed was 10 wt.% and 2.5 wt.%, respectively. In the second series, with 24 g of oxygen carrier in the bed, the reducing periods consisted of introducing loads of coal from 0.4 to 1.2 g, i.e. the oxygen carrier to coal ratio was in the range 60-20. Further, in the third series (with only 6 g of oxygen carrier in the bed) the loads of coal change from 0.03 to 0.5 g, corresponding to oxygen carrier to coal ratios of 200 and 12, respectively. In this way, the oxygen carrier to carbon mass ratio was decreased

but a mass of coal higher than 2 g was not used. 2 g was the highest amount of coal that could be feed to obtain repetitive and useful results. Higher mass of coal resulted in relevant entrainment of solids originated by the big amount of gases generated.

For the coal and oxygen carrier material used in this work the stoichiometric oxygen carrier to coal ratio is 30. At this condition, the exact amount of oxygen to fully convert coal to CO₂ and H₂O is present in the particles. For lower oxygen carrier to coal ratios, some char will remain unconverted at the end of the reduction period. However, tests working with lower ratios were accomplished to evaluate the maximum value of the instantaneous oxygen generation rate of the oxygen carrier. In the batch fluidized bed, the unconverted char was burnt during the oxidation period. However, in a continuously operated CLOU system, the depleted oxygen particles should be replaced with particles coming from the air reactor, thus avoiding the limitation in the oxygen availability happening in a batch fluidized-bed reactor. But the behaviour of the oxygen carrier against coal combustion in the batch reactor would be similar to that in a CLOU unit.

An additional series was done using char instead of coal as fuel. This series of experiments was carried out with an oxygen carrier mass fraction of 2.5 wt.%. The char loads changed from 0.04 to 0.4 g, corresponding to oxygen carrier to char mass ratios of 150 and 14, respectively.

2. Data evaluation

To analyze the oxygen uncoupling properties of the Cu60MgAl oxygen carrier, consecutive redox cycles have been done in a batch fluidized-bed reactor. During the reduction period a batch of coal was added to the bed, whereas oxidation with air was accomplished during the oxidation period. The instantaneous rate of oxygen generation per amount of oxygen carrier, $r_{O_2,red}(t)$, was calculated from a mass balance to the oxygen atoms in the reactor.

$$r_{O_2,red}(t) = \frac{M_{O_2}}{m_{OC}} \left[F_{O_2} + F_{CO_2} + 0.5(F_{CO} + F_{H_2O}) - 0.5F_{O,coal} \right] \quad (6)$$

The molar gas flow of each component exiting the fuel reactor, F_i , is calculated as:

$$F_i = F_{out} \cdot y_i \quad (7)$$

F_{out} being total dry basis outlet flow calculated by using the N_2 flow to the reactor, F_{N_2} .

$$F_{out} = \frac{F_{N_2}}{(1 - \sum_i y_i)} \quad (8)$$

y_i is the molar fraction of the component i in the product gas analyzed in every experimental condition. Possible gas i includes O_2 , CO_2 , CO , H_2 and CH_4 . Nevertheless, methane and hydrogen were not considered in the balance because they were not detected in any case. The water concentration was not measured. However, to consider the oxygen exiting with H_2O coming from oxidation of hydrogen in the coal, it was assumed that the hydrogen evolution was proportional to the carbon evolution, maintaining the same C/H ratio in the gases than in the coal. Thus, the H_2O flow was calculated as:

$$F_{H_2O} = 0.5 f_{H/C} (F_{CO_2} + F_{CO}) \quad (9)$$

$f_{H/C}$ being the hydrogen to carbon molar ratio in coal ($f_{H/C} = 0.61$, for Colombian pre-treated coal). Equally, the evolution of oxygen from coal was assumed to be proportional to coal evolution. Thus, the flow of oxygen coming from coal, $F_{O,coal}$ in Eq. (7), was calculated as:

$$F_{O,coal} = f_{O/C} (F_{CO_2} + F_{CO}) \quad (10)$$

$f_{O/C}$ being the oxygen to carbon molar ratio in the coal ($f_{O/C} = 0.20$, for Colombian pre-treated coal).

When char was used as fuel, a conversion rate of char per mass of reacting char in the reactor was calculated as the rate of carbon combustion to give CO_2 or CO :

$$(-r_{char}(t)) = \frac{F_{CO_2} + F_{CO}}{\frac{m_{char} \cdot f_{C,char}}{M_C} - \dot{O}_0 (F_{CO_2} + F_{CO}) dt} \quad (11)$$

m_{char} being the mass of char in the fuel batch and $f_{C,char}$ the carbon content in char.

Before starting a reducing period, the oxygen carrier particles were fully oxidized, i.e. the oxygen carrier conversion was $X_o = 1$. As the oxygen carrier particles were reacting during reduction period, the oxidation degree decreased. Thus, the oxygen carrier conversion was calculated from the integration of $r_{O_2,red}$ with time:

$$X_o(t) = 1 - \frac{1}{N_{O_2}} \int_0^t r_{O_2,red}(t) dt \quad (12)$$

N_{O_2} being the molar amount of oxygen in the oxygen carrier active for CLOU process, i.e. from reduction of CuO to Cu₂O expressed as molar O₂:

$$N_{O_2} = \frac{m_{OC} R_{OC}}{M_{O_2}} \quad (13)$$

Thus, the final conversion of the particles, X_o , was calculated by integrating Eq. (12) for the time spent in reduction conditions. In the same way, an oxygen balance was done to calculate the oxidation rate with air –Eq. (14)– and the evolution with time of the oxygen carrier conversion, X_o –Eq. (15)–. In some cases, char was not completely converted during the reduction period because the depletion of oxygen in the particles was reached. Thus, CO₂ and CO can appear during the oxidation period as the remaining char is burned with oxygen in air, being the oxygen for char combustion considered in Eq. (14).

$$(-r_{O_2,ox}(t)) = \frac{M_{O_2}}{m_{OC}} \left[0.21F_{air} - F_{O_2} - (F_{CO_2} + 0.5F_{CO}) \right] \quad (14)$$

$$X_o(t) = X_{o,f} + \frac{1}{N_{O_2}} \int_0^t (-r_{O_2,ox}(t)) dt \quad (15)$$

Finally, the CO₂ yield was defined as the carbon fraction as CO₂ in the outgoing gases, calculated as:

$$\gamma_{CO_2} = \frac{F_{CO_2}}{F_{CO_2} + F_{CO}} \quad (16)$$

3. Results

Reduction-oxidation multi-cycles with Cu60MgAl oxygen carrier were carried out in a batch fluidized-bed reactor to determine the oxygen release behaviour as a function of the operating conditions in similar environment to that found in a CLOU process with solid fuels. Moreover, the fluidization behaviour of the solid particles with respect to the agglomeration phenomena could be observed.

Test series were carried out by using different bed materials: first, the bed material was Cu60MgAl particles; second, the bed material was 10 wt.% oxygen carrier diluted in alumina particles; and third, only 2.5 wt.% Cu60MgAl diluted in alumina. All these tests were carried out with a total mass of particles in the reactor of 240 g. The oxygen carrier was subjected to about 34 redox cycles which last during 31 h between 900 to 950 °C. The oxygen carrier never showed agglomeration problems, even when the oxygen carrier was highly reduced to Cu₂O during the reduction period.

Fig. 4 shows the concentration of O₂, CO₂ and CO measured at the outlet of the reactor and the bed temperature during a typical reduction and oxidation cycle at 925 °C with an oxygen carrier inventory in the reactor of 240 g. The fluidizing medium was pure nitrogen during reduction and during oxidation the inlet oxygen concentration was 21 vol.%. The time $t = 0$ corresponds to the initial time of the reduction period, i.e. when air during oxidation was replaced by nitrogen. At the beginning a rapid oxygen release occurred close to the oxygen concentration equilibrium for the measured bed temperature. After a short period, a batch of 2 g of coal particles were fed to the reactor, and only CO₂ and O₂ were observed in the outgoing gases, indicating full combustion of the volatiles and char. The CO₂ concentration in this case was as high as 76 vol.% which was maintained constant during ~8 s, and eventually decreased to zero when the complete coal combustion was reached. This result suggests a fast combustion of coal where it is not differentiated a first period of fast combustion of volatiles from a subsequent slower period of combustion of the remaining char. At this condition, the gas flow at the reactor exit was increased by a factor of 5 with regard to the inlet N₂ flow because the CO₂ and H₂O generated during coal combustion.

In addition, the oxygen release rate was high enough to supply an excess of gaseous oxygen (O₂) exiting together the combustion gases. During coal combustion the bed temperature increased about 30 °C due to the exothermic reaction of CuO with coal, see Eq. (5). The oxygen concentration was correspondingly increased, remaining close to the equilibrium condition when temperature varied. This fact indicates that the oxygen carrier was able to transfer the oxygen demanded by the coal combustion and even more gaseous oxygen until equilibrium was reached. Therefore, the conversion of coal was limited by the coal reactivity, i.e. by the coal combustion rate at the existing oxygen concentration in the bed. It must be taking into account that in the fuel reactor two processes in series are happening: oxygen generation and coal combustion with the oxygen generated. If oxygen generation rate is

higher than rate of coal combustion, oxygen at equilibrium is reached, and the coal combustion rate depends on the coal reactivity. On contrary, the oxygen at equilibrium is not reached and the coal combustion rate will be limited by the oxygen generation rate.

In Fig. 4, the variation of oxygen carrier conversion, X_o , with reacting time is also shown. It can be seen that the oxygen carrier was slowly converted during the initial period before coal addition. Besides, the oxygen carrier was able to produce gaseous oxygen until the equilibrium concentration was reached. Therefore, the oxygen generation rate was limited by the fact that the equilibrium concentration is reached in absence of fuel. A sharp decrease in the oxygen carrier conversion was happening when coal was fed to the reactor because the fast oxygen transference from oxygen carrier to fuel. After coal was completely burnt the temperature decreased until the set point value. As the oxygen carrier was not completely reduced after coal combustion, still oxygen was generated up to equilibrium concentration was reached. The variation in the solids conversion during the reducing period was 41%. Then, oxidation period starts at $t = 360$ s and a quick increase in the temperature occurred due to the highly exothermic reaction. Equally to reduction period, oxygen concentration was close to the equilibrium condition until the oxygen carrier was fully oxidized, which is in accordance to highly reactive materials observed in TGA experiments [20, 21].

Similar behaviour was observed in redox cycles when different amounts of coal were added to the bed in the range 0.2-2.0 g, corresponding to oxygen carrier to coal ratios between 1200 and 120. As expected, the CO_2 concentration from fuel reactor increased with the coal mass added because more fuel is burnt. Also, more oxygen is transferred to gases. CH_4 , CO or H_2 were not observed in any case, indicating the full combustion of volatiles in the bed, as well as carbon in char. From the CO_2 and O_2 evolution in the gas phase, it was possible to calculate the instantaneous oxygen generation rate, $r_{\text{O}_2, \text{red}}$, from Eq. (6). The higher value of $r_{\text{O}_2, \text{red}}$ was obtained when coal was added to the bed, and it was maintained roughly constant while the coal combustion proceeds. Fig. 5 shows the instantaneous oxygen generation rate during the coal combustion period, $r_{\text{O}_2, \text{red}}$, as a function of the oxygen carrier to coal mass ratio. In all cases the ratio of oxygen carrier to coal is above the stoichiometric value to convert coal to CO_2 and H_2O . The effect of the oxygen carrier to coal ratio is evident on the oxygen generation rate. In this case it is observed that $r_{\text{O}_2, \text{red}}$ is inversely proportional to the oxygen carrier to coal ratio. The incremental oxygen requirements when the batch of coal increases

(i.e. the oxygen carrier to coal is decreased) is fully provided by the oxygen carrier. Thus, at the CLOU conditions used in these experiments, the oxygen generated in the reactor was not limited by the reactivity of the oxygen carrier but for the demand of oxygen by coal; i.e. the more oxygen is demanded, the more oxygen is supplied. This fact suggests that a decrease in the oxygen carrier to coal ratio would allow increasing the oxygen generation rate provided by the Cu60MgAl oxygen carrier. Thus, the maximum in the instantaneous oxygen generation rate by this material could not be observed during these series of experiments, being necessary to work with higher values of oxygen carrier to coal ratios. However, the reproducibility of results in the fluidized bed failed with coal batches higher than 2 g which conducted to a loss in the confidence of the calculated oxygen generation rate.

In order to decrease the oxygen carrier to coal ratio but still maintain the confidence on the results obtained, the following tests were carried out diluting the oxygen carrier in alumina particles, but keeping the total mass of solids in the reactor to be 240 g. Firstly, batches of coal in the range 0.4-1.2 g were used at 925 °C using an oxygen carrier mass fraction of 10 wt.% in alumina. Then, the oxygen carrier to coal ratio was in the range 60-20. During the experimental work it was observed that for oxygen carrier to coal ratios lower than 35 the oxygen carrier was fully reduced after coal addition whereas char remained unburnt. Thus, some unconverted char was burnt in the subsequent oxidation period, which was evidenced by the presence of CO₂ in the gases when air was introduced to the bed. The value of oxygen carrier to coal of 35 was close to the stoichiometric oxygen available in the bed material to convert the coal to CO₂ and H₂O, which was an oxygen carrier to coal ratio of 30. The oxygen carrier to coal value observed during experimental work was some higher because some oxygen in particles was evolved to gas before coal addition to the bed.

During the time converting coal, similar behaviour to that found when using only Cu60MgAl particles as bed material was observed in the oxygen carrier to coal range of 60-50. Further decrease in the oxygen carrier to coal ratio below 50 caused the appearance of CO together with CO₂ in the exhaust gases during the reduction period, as well as lower oxygen concentration compared to the equilibrium concentration. Nevertheless, CH₄ or H₂ were not found in any case. This fact indicates that the instantaneous oxygen generation rate is approaching to the maximum value given by the reactivity of the oxygen carrier.

Fig. 6(a) shows the CO₂ yield, γ_{CO_2} , whereas the ratio between the oxygen concentration at the reactor exit and that present at equilibrium conditions, $O_2/O_{2,eq}$, was plotted in Fig. 6(b). It can be seen as both the CO₂ yield and the oxygen concentration decreases when the oxygen carrier to coal mass ratio was lower than ~50. This behaviour is due to that the oxygen carrier is not able to release oxygen fast enough to fully burnt coal to CO₂, although over-stoichiometric conditions are used.

O₂ and CO were both found in the gaseous stream exiting the reactor, because the oxygen concentration in the gases was too low to allow the full combustion of CO to CO₂. The amount of oxygen in the flue gases would be enough to convert the remaining CO to CO₂ for oxygen carrier to coal ratios higher than 35, but this has not happened in the reactor. However, an excess of CO regarding the O₂ present in gases was found for oxygen carrier to coal ratios lower than 35. At these conditions, if conversion of CO to CO₂ was desired in a down-stream step, addition of oxygen should be done to the exiting stream.

Fig. 7 shows the oxygen generation rate as a function of the oxygen carrier to coal ratio when the Cu60MgAl particles were 10 wt.% diluted in alumina. In the same way that in the previous tests, the oxygen generation rate increased as the oxygen carrier to coal ratio decreased. This fact suggests that the presence of CO in the outgoing gases was not due to a limitation of the oxygen carrier to supply the required oxygen by the fuel, but rather to an inefficient combustion of char or volatiles at the low oxygen concentrations. The lower oxygen concentration than the equilibrium value would indicate that the oxygen generation rate is reaching its maximum value given by the oxygen carrier reactivity.

An attempt to determine the maximum oxygen generation rate of the Cu60MgAl material was done in a third series of experiments. In these tests an additional dilution of the oxygen carrier material in alumina was done. So, the mass fraction of the Cu60MgAl was 2.5 wt.%, whereas the loads of coal were between 0.03 and 0.5 g, corresponding to oxygen carrier to coal ratios from 200 to 12. Fig. 8 shows the oxygen generation rate as a function of the oxygen carrier to coal ratio in a double logarithmic scale. To observe the global trend of the oxygen generation rate, the previous results obtained with different dilutions of the oxygen carrier in alumina, i.e. 100 wt.% and 10 wt.%, were included and plotted. It can be observed a similar trend of the data obtained with different oxygen carrier dilutions at similar oxygen carrier to coal ratios. When the oxygen carrier to coal ratio decreased from high values until a value of 25, the

oxygen generation rate increased. However, at lower oxygen carrier to coal values it seemed that the oxygen generation rate reached a maximum, and no further incremental in the oxygen generation rate was obtained by decreasing the oxygen carrier to coal ratio. Thus, for oxygen carrier to coal < 25 -where the maximum rate for oxygen generation was reached- the coal conversion was limited by the oxygen generation rate from the oxygen carrier. The calculated value for the maximum oxygen generation rate was $2.6 \cdot 10^{-3}$ kg O₂/s per kg of oxygen carrier when the temperature during the reduction period increased up to 955 °C.

The CO₂ yield and the O₂/O_{2,eq} ratio obtained for the third experimental series were also shown in Fig. 6(a) and 6(b), respectively. Both, the CO₂ yield and the O₂/O_{2,eq} ratio followed a downward trend when the oxygen carrier to coal ratio decreased. Moreover, the oxygen concentration becomes zero when the maximum rate of oxygen generation was reached. This fact determines a change in the limiting process during conversion of coal from the rate of coal combustion determined by the char reactivity towards the rate of oxygen production by the oxygen carrier determined by the oxygen carrier reactivity.

Analogous experiments were carried out at initial temperatures, T_0 , of 900 °C and 950 °C. In these cases, temperature increased until T_{max} of 930 °C and 980 °C, respectively, when coal was added to the bed. Similar trend was found for the oxygen generation rate with the oxygen carrier to coal ratio. Nevertheless, the maximum oxygen generation rate increased with the reacting temperature, as showed in Table 3.

In the second and third experimental series, it can be observed that with an oxygen carrier to coal ratio lower than 50, CO was present in the outlet gases from the reactor. The presence of CO could come from unconverted volatiles in the bed or from char combustion, since a relevant amount of CO can appear as combustion product of solid fuels in an oxygen lean atmosphere [28]. To evaluate the CO source an experimental series was done using char instead of coal. The oxygen carrier to char mass ratios varied from 150 to 14. Similar to experiments with coal, gaseous oxygen was in the gases at equilibrium concentration for high oxygen carrier to coal mass ratios. But in this case, the oxygen concentration decreased for oxygen carrier to char mass ratio below 130 becoming zero at oxygen carrier to char ratios lower than 50. In all the experiments carried out with char no CO was present in the outlet gases even if oxygen was not present in the exhaust gases. This fact suggests that the CO detected in test with coal at oxygen carrier to coal ratios lower than 50, was due to unburnt

volatiles. The presence of CO could be due to the oxygen transference rate from the oxygen carrier was not fast enough to fully convert carbon in volatiles to CO₂, but oxygen remaining in the oxygen carrier is able to burn char fast enough to CO₂.

Fig. 9 shows the oxygen generation rate as a function of oxygen carrier to fuel mass ratio when coal or char were burnt with Cu₆₀MgAl particles 2.5 wt.% diluted in alumina. It can be observed that at oxygen carrier to fuel ratios higher than 100 oxygen generation rates were similar both for coal and char. However, when the oxygen carrier to fuel ratio decreased, oxygen generation rate in the case of coal is 2 times higher than when the fuel is char. When char was used as fuel, the maximum oxygen generation rate obtained was the same than the value found by thermo-gravimetric analysis during CuO decomposition in N₂ [20, 21]. Thus, the maximum reaction rate using char in the fluidized bed looks to be the maximum rate of generation of gaseous oxygen from particles, which is the same than that obtained in TGA. At low oxygen carrier to coal ratios, oxygen was not present. So, the maximum rate of oxygen generation was reached for this condition due to the driving force, i. e. the difference between the partial pressure of oxygen at equilibrium and the oxygen in the phase, is maximum. The highest oxygen generation rate obtained when coal was burnt could be explained by the direct reduction of CuO by the volatile matter. In this case, gas-solid reaction between volatile matter and oxygen carrier could be faster than oxygen generation rate. In this way, the rate of transference of oxygen from solid particles to gaseous compounds (O₂, CO₂, H₂O or CO) is faster when coal is used instead of char. More studies are needed to confirm this explanation.

In the fuel reactor of a CLOU process, two processes should happen in series: oxygen generation and coal combustion with the oxygen generated. Also, the gas-solid reaction between reacting gases, e.g. volatile compounds, and the solid oxygen carrier could be relevant. The oxygen generation rate has been analyzed as much with coal as char. Differences were attributed to the presence of volatiles in coal. Now, an analysis about the rate of char combustion is done. With the results obtained using char as fuel it can be calculated the char combustion rate. Fig. 10 shows the char combustion rate as a function of the oxygen carrier to char ratio at 925 °C when Cu₆₀MgAl particles were 2.5 wt% diluted in alumina. The char combustion rate increased with the oxygen carrier to char ratio up to a maximum. This maximum in the char combustion rate was reached at oxygen carrier to char ratios higher than 100. At lower ratios the conversion rate of char was limited by the rate of oxygen supply from the oxygen carrier. At oxygen carrier to char ratios higher than 100 the

oxygen availability is not limited by oxygen carrier reactivity. Thus, all the oxygen demanded for char combustion is supplied by the oxygen carrier at enough high rate, and the combustion rate of char is fixed by its own reactivity with oxygen and the oxygen concentration in the reactor. The oxygen concentration during char combustion is determined by thermodynamic equilibrium of CuO decomposition to Cu₂O. The maximum char combustion rate reached was 3.12 %/s at the maximum temperature reached during the experiment, i.e. $T_{\max} = 955$ °C. This value is 10 times lower to that obtained during coal continuous combustion in a CLOU unit [16] (27 %/s at 960 °C). This fact may be explained due to the char used in this work is much less reactive than the nascent char produced in the direct combustion of the coal. The relevance of the thermal treatment on the char reactivity in combustion or gasification processes is a well known behaviour [29-32], which supports these results.

4. Discussion

The rate of oxygen generation calculated by the procedure above described can be related to the solids inventory needed to fully convert the fuel in the fuel reactor of a CLOU system. Assuming that the solids circulation rate in a CLOU system is high enough to transport the required oxygen in the fuel reactor, the coal combustion would be not limited by the availability of oxygen transported from the air reactor. Thus, the solids inventory, m_{FR} , depends on the flow of coal that the oxygen carrier is able to process at the rate of oxygen generation assumed, $r_{O_2,red}$, and it can be calculated as:

$$m_{FR} = 10^3 \frac{m_O}{r_{O_2} LHV} \quad (17)$$

being m_O the mass of oxygen required per kg of coal to fully convert it to CO₂ and H₂O, as for the case of the conventional combustion with air. LHV is the lower heating value of the solid fuel. From coal analysis showed in Table 2, a value for $m_O = 2.1$ kg O₂ per kg of coal was calculated, whereas the LHV was 25878 kJ/kg for pre-treated “El Cerrejón” coal. Notice that the solids inventory does not depends on the oxygen carrier to coal ratio in experiments, but depends on the oxygen generation rate obtained.

The calculated solids inventories for the maximum oxygen generation, r_{O_2} , are shown in Table 3. The solids inventory in the fuel reactor was dependent on the reactor temperature

because the increase of the oxygen generation rate with the temperature. Thus, 39 kg/MW_{th} would be necessary in the fuel reactor at a reacting temperature of 930 °C, decreasing to 29 kg/MW_{th} if temperature increases up to 980 °C. Here, the temperature is the maximum temperature reached during the reduction period.

These values of solids inventory corresponds to the minimum amount of solids that generate the required oxygen for coal combustion but not having an excess of oxygen in the gases. However, from the experimental results it seems that an excess of oxygen in the exhaust gases must be necessary in order to reach complete combustion of fuel to CO₂ and H₂O. Thus, the maximum generation rate of oxygen was obtained for oxygen carrier to coal ratios lower than 25, but incomplete combustion of coal can happen with CO at the outlet stream for oxygen carrier to coal ratios lower than 50. This fact would reduce the combustion efficiency if solids inventories showed in Table 3 were used, which corresponded to the calculated values using the maximum oxygen generation rate. In order to increase the combustion efficiency, the complete combustion of gases can be addressed improving the contact time between the oxygen carrier and unburnt CO in gases, e.g. increasing the solids inventory in the fuel reactor. Thus, higher solids inventory than that calculated using the maximum rate of oxygen generation could be necessary in order to get complete combustion of fuel to CO₂ and H₂O.

From the results obtained in this work, three different regions for coal combustion in the CLOU process can be identified depending on the oxygen carrier to coal ratio. Fig. 11 shows the delimiting conditions for these regions and the calculated solids inventory. The solids inventory depends on the instantaneous rate of oxygen generation obtained for every value of oxygen carrier to carbon mass ratio. The Region I was defined as the region where CO was not present in the exhaust gases, corresponding to oxygen carrier to coal ratios higher than 50. The oxygen generation rate for the delimiting border was about $1.4 \cdot 10^{-3}$ kg O₂/s per kg of oxygen carrier corresponding to a solid inventory of 58 kg/MW_{th}. In the Region II, O₂ and CO simultaneously appeared in the outgoing gases. This region is limited between values of oxygen carrier to coal ratios of 25 and 50, and it can be divided in two: at higher oxygen carrier to coal ratios than 35, the fraction of oxygen in gases was enough to convert the existing CO to CO₂, and even an excess of oxygen remained in gases. At this condition, the oxygen generation rate was about $1.9 \cdot 10^{-3}$ kg O₂/s per kg of oxygen carrier corresponding to a solid inventory of 43 kg/MW_{th} at 955 °C. Thus, in the range 43-58 kg/MW_{th} complete combustion could be accomplished downstream in a subsequent step by catalytic combustion

without addition of new O_2 . Finally, in the Region III no oxygen was present in the exhaust gases. The maximum rate for oxygen generation of the oxygen carrier is reached, and lowering the solids inventory does not allow supplying oxygen to fully convert the coal in the fuel reactor at the rate that is demanded by the coal feeding rate. This region was observed for oxygen carrier to coal ratios lower than 25.

In this work, the dependence of the oxygen generation rate on the oxygen carrier to coal ratio was analyzed to obtain the maximum rate of O_2 release. The numbers of the oxygen carrier to coal ratios defining the regions in this work are for the Colombian pre-treated coal. These numbers could be different as function of the fuel, that is, the ratio needed to reach the maximum rate would depend on reactivity of coal and its composition. Thus, the more reactive is a coal, the more oxygen carrier to coal ratio would be needed to reach this maximum. This fact is explained because as the solid fuel is more reactive, a lower amount of solid fuel would be needed to demand oxygen at the same rate.

From the results showed in this work, it can be concluded that a small oxygen amount is desirable in the flue gases coming from the fuel reactor if complete combustion wants to be reached. In this way, the necessity of an oxygen polishing step would be avoided. Thus, it can be suggested that a CLOU system should be operated in the Region I, where complete combustion of coal can be obtained. It is necessary to notice that this does not mean all coal would be converted to gas, but all gas produced from coal is oxidized to CO_2 and H_2O . Depending on the char reactivity and the residence time in the reactor, some char will be transferred to the air reactor before it was converted. If a relevant fraction of char was bypassed to the air reactor, a higher mean residence time of solids should be necessary in the fuel reactor. This can be accomplished or (1) by increasing the solids inventory in the fuel reactor; or (2) by introducing a carbon separation system between the fuel reactor and the air reactor, which separates char from oxygen carrier particles to be recirculated to the fuel reactor. In this case, the solids inventory calculated in this work should be the lowest amount of solids required to fully convert coal.

The excess of oxygen in Region I should decrease as the fuel reactor temperature was lower because the oxygen concentration at equilibrium is reduced. It is remarkable that the excess of oxygen could be problematic for the transport and storage of the CO_2 , and it must be removed from the exhaust gas stream. This situation is similar to that present in coal oxy-combustion

units. To address the excess of oxygen, one option would be to separate the oxygen in the purification and compression process of the CO₂ before being transported [33].

5. Conclusions

A Cu-based oxygen carrier prepared by spray drying was tested for the CLOU process in a batch fluidized-bed reactor. The oxygen carrier containing CuO (60 wt.%) and MgAl₂O₄ was used as inert material, whereas the bituminous Colombian coal “El Cerrejón” was used as fuel. The capability of particles to evolve gaseous oxygen in the fuel reactor was evaluated as a function of the oxygen carrier to coal mass ratio and reactor temperature. The oxygen carrier was subjected to about 34 redox cycles which last during 31 h between 900 to 950 °C. The oxygen carrier never showed agglomeration problems during all the experimental work.

A decrease in the oxygen carrier to coal mass ratio caused a continuous increase in the oxygen generation rate of the Cu60MgAl material until the maximum rate of oxygen generation was reached. The maximum generation rate obtained with coal was higher (about twice) the reaction rate obtained with char. Results obtained with char were representative of the rate of evolution of gaseous oxygen from particles, whereas experiments with coal also could include a fast gas-solid reaction rate between volatile matter and solid particles with direct reduction of CuO.

The oxygen generation rate was related to the solids inventory in the fuel reactor in a CLOU process. Three operating regions were identified depending on the solids inventory. Unburnt compounds were not present in the outgoing gases in Region I when the calculated solids inventory was higher than 58 kg/MW_{th} at 955 °C. CO₂ and H₂O were the only products of coal combustion and an excess of O₂ was observed, which was found to be close to the equilibrium concentration. At these conditions, the oxygen concentration at the reactor outlet increased with the temperature. The Region II was confined between 32 and 58 kg/MW_{th}, where both CO and O₂ were present in the exhaust gases together CO₂ as main product. CO was the only unconverted product present in gases, which came from incomplete oxidation of volatile matter. The maximum rate of oxygen generation was found in the so-called Region III. Oxygen was not present in the flue gases, and a certain concentration of CO was present as unburnt compound. Maximum oxygen generation rates from $2.1 \cdot 10^{-3}$ at 930 °C to $2.8 \cdot 10^{-3}$ kg O₂/s per kg of oxygen carrier at 980 °C were found. The estimated solids inventory in the

fuel reactor changed from 39 at 930 °C to 29 kg/MW_{th} at 980 °C. However, for full combustion of coal to CO₂ and H₂O a minimum bed inventory of 43 kg/MW_{th} at 930 °C was necessary, corresponding to a zone in Region II where oxygen released from the reactor is enough to convert CO to CO₂ in the exhaust gases.

The results obtained in this work showed that the reactivity of the Cu60MgAl oxygen carrier allows the complete conversion of the solid fuel in a CLOU process with very low solids inventory and avoiding the oxygen polishing step. The method proposed in this work can be used for other oxygen carrier materials and coals in order to compare the behaviour of different materials in the CLOU process.

Acknowledgement

This work was partially supported by the European Commission, under the RFCS program (ECLAIR Project, Contract RFCP-CT-2008-0008), ALSTOM Power Boilers (France) and by the Spanish Ministry of Science and Innovation (PN, ENE2010-19550). I. Adánez-Rubio thanks CSIC for the JAE fellowship co-funded by the European Social Fund.

6. Nomenclature

$f_{C, char}$	mass fraction in char of carbon (-).
$f_{H/C}$	hydrogen to carbon molar ratio in the coal (-)
$f_{O/C}$	oxygen to carbon molar ratio in the coal (-)
F_{air}	molar flow of air (mol/s)
F_i	molar flow of gas i (mol/s)
F_{out}	molar flow at the reactor exit (mol/s)
$F_{O, coal}$	molar flow of oxygen from the existing oxygen in the coal (mol/s)
m_{char}	mass of char fed to the fuel reactor (kg)
m_{FR}	mass of oxygen carrier in the fuel reactor (kg/MW _{th})
m_O	mass of oxygen required per kg of coal to complete combustion (kg O ₂ /kg coal)
m_{ox}	mass of fully oxydized oxygen carrier (kg)
m_{OC}	mass of oxygen carrier in the reactor (kg)
m_{red}	mass of reduced oxygen carrier, as Cu ₂ O (kg)
M_C	molecular weight of carbon (=12·10 ⁻³ kg/mol)
M_{O_2}	molecular weight of oxygen (=32·10 ⁻³ kg/mol)
N_{O_2}	amount of oxygen, expressed as O ₂ , in the bed material (mol)
r_{char}	rate of char combustion (kg C/s per kg C)
$r_{O_2, red}$	rate of oxygen generation in the reduction (kg O ₂ /s per kg of oxygen carrier)
$r_{O_2, ox}$	rate of oxygen consumption in the oxidation (kg O ₂ /s per kg of oxygen carrier)
$r_{O_2, max}$	maximum rate of oxygen generation (kg O ₂ /s per kg of oxygen carrier)
ROC	oxygen transport capability (-)
t	time (s)
T	temperature (°C)
T_0	initial temperature in the experiment (°C)
T_{max}	maximum temperature reached during experiment (°C)
X_o	oxygen carrier conversion (-)
X_{of}	oxygen carrier conversion at the end of the reducing period (-)
y_i	molar fraction of gas i (-)

Greek symbols

ΔH_r Enthalpy of reaction (kJ/mol)

γ_{CO_2} CO₂ yield (-)

Acronyms

LHV Low Heating Value (kJ/kg)

OC Oxygen carrier

7. References

- [1] IPCC. IPCC special report on carbon dioxide capture and storage. Working group III of the intergovernmental panel on climate change. Cambridge: Cambridge University Press, U.K.; 2005 (available at <http://www.ipcc.ch>).
- [2] Kerr HR. Capture and Separation Technology Gaps and Priority Research Needs. Carbon Dioxide Capture for Storage in Deep Geologic Formations. Amsterdam: Elsevier Science; 2005, p. 655-660.
- [3] Kvamsdal HM, Jordal K, Bolland O. A quantitative comparison of gas turbine cycles with CO₂ capture. *Energy* 2007;32(1):10-24.
- [4] Kolbitsch P, Bolh ar-Nordenkamp J, Pr oll T, Hofbauer H. Comparison of two Ni-based oxygen carriers for chemical looping combustion of natural gas in 140 kW continuous looping operation. *Industrial & Engineering Chemistry Research* 2009; 48(11):42-7.
- [5] Linderholm C, Mattisson T, Lyngfelt A. Long-term integrity testing of spray-dried particles in a 10 kW chemical-looping combustor using natural gas as fuel. *Fuel* 2009;88:2083-96.
- [6] Ad anez J, Gay an P, Celaya J, de Diego LF, Garc a-Labiano F, Abad A. Chemical looping combustion in a 10 kW_{th} prototype using a CuO/Al₂O₃ oxygen carrier: effect of operating conditions on methane combustion. *Industrial & Engineering Chemistry Research* 2006; 45(17):75-80.
- [7] Lyngfelt A, Thunman H. Construction and 100 h of operational experience of a 10-kW chemical-looping combustor. In: Thomas DC, Benson SM, editors. Carbon dioxide capture for storage in deep geologic formations– Results from the CO₂ capture project, Oxford, UK: Elsevier; 2005, vol. 1, Chapter 36.
- [8] Pr oll T, Mayer K, Bolh ar-Nordenkamp J, Kolbitsch P, Mattisson T, Lyngfelt A, Hofbauer H. Natural minerals as oxygen carriers for chemical looping combustion in a dual circulating fluidized bed system. *Energy Procedia* 2009;1:27-34.
- [9] Ad anez J, Abad A, Garc a-Labiano F, Gay an P, de Diego LF. Progress in Chemical-Looping Combustion and Reforming Technologies. *Prog. Energy Comb. Sci.* 2012, 38:215-282.

Con formato: Ingl es (Estados Unidos)

- [10] Cao Y, and Pan WP. Investigation of chemical looping combustion by solid fuels. 1. Process analysis. *Energy&Fuel* 2006;20:57-68.
- [11] Cuadrat A, Abad A, García-Labiano F, Gayán P, de Diego LF, Adánez J. Effect of operating conditions in Chemical-Looping Combustion of coal in a 500 W_{th} unit. *Int J Greenhouse Gas Control* 2012;6:153-63.
- [12] Berguerand N, and Lyngfelt A. Chemical-Looping combustion of petroleum coke using ilmenite in a 10 kW_{th} unit-High-temperature operation. *Energy&Fuel* 2009; 23:57-68.
- [13] Mattisson T, Lyngfelt A, Leion H. Chemical-looping oxygen uncoupling for combustion of solid fuels. *Int J Greenhouse Gas Control* 2009;3:11-19.
- [14] Lewis WK, Gilliland ER. Production of pure carbon dioxide. Patent 2665972; 1954.
- [15] Mattisson T, Leion H, Lyngfelt A. Chemical-Looping with Oxygen Uncoupling using CuO/ZrO₂ with petroleum coke. *Fuel* 2009;88:683-90.
- [16] Abad A, Adánez-Rubio I, Gayán P, García-Labiano F, de Diego LF, Adánez, J. Demonstration of chemical-looping with oxygen uncoupling (CLOU) process in a 1.5 kW_{th} continuously operating unit using a Cu-based oxygen-carrier. *Int. J of Greenhouse Gas Control* 2012;6:189-200.
- [17] Leion H, Mattisson T, Lyngfelt A. Using chemical-looping with oxygen uncoupling (CLOU) for combustion of six different solid fuels. *Energy Procedia* 2009;1:447-53.
- [18] Eyring E, Konya G, Lighty J, Sahir A, Sarofim A, Whitty K. Chemical looping with copper oxide as carrier and coal as fuel. *Oil & Gas Science and Technology- Revue IFP Nouvelles Technologies* 2011;2:209-21.
- [19] HSC Chemistry 6.1® 2008. Chemical Reaction and Equilibrium Software with Thermochemical Database and Simulation Module. Outotec Research Oy.
- [20] Adánez-Rubio, I.; Gayán, P.; García-Labiano, F.; de Diego, L.F.; Adánez, J.; Abad, A. Development of CuO-based oxygen-carrier materials suitable for Chemical-Looping with Oxygen Uncoupling (CLOU) process. *Energy Procedia* 2011;4:417-24.
- [21] Gayán P, Adánez-Rubio I, Abad A, de Diego LF, García-Labiano F, Adánez, J. Development of CuO-based oxygen-carrier materials suitable for Chemical-Looping with Oxygen Uncoupling (CLOU) process. *Fuel* 2012;6:226-38.

- [22] Shulman A, Cleverstam E, Mattisson T, Lyngfelt A. Manganese/iron, manganese/nickel, and manganese/silicon oxides used in chemical looping with oxygen uncoupling (CLOU) for combustion of methane. *Energy Fuels* 2009;23:5269-75.
- [23] Azimi G, Leion H, Mattisson T, Lyngfelt A. Chemical-looping with oxygen uncoupling using combined Mn-Fe oxides, testing in batch fluidized bed. *Energy Procedia* 2011;4:370-7.
- [24] Rydén M, Lyngfelt A, Mattisson T. Combined manganese/iron oxides as oxygen carrier for chemical-looping combustion with oxygen uncoupling (CLOU) in a circulating fluidized bed reactor system. *Energy Procedia* 2011;4:341-8.
- [25] Leion H, Larring Y, Bakken E, Bredesen R, Mattisson T, Lyngfelt A. Use of $\text{CaMn}_{0.875}\text{Ti}_{0.125}\text{O}_3$ as oxygen carrier in chemical looping with oxygen uncoupling. *Energy Fuels* 2009;23:5276-83.
- [26] Rydén M, Lyngfelt A, Mattisson T. $\text{CaMn}_{0.875}\text{Ti}_{0.125}\text{O}_3$ as oxygen carrier for chemical oxygen combustion with oxygen uncoupling (CLOU) – Experiments in a continuously operating fluidized-bed reactor system. *Int J of Greenhouse Gas Control* 2010.;5: 356-66.
- [27] Pis JJ, Centeno TA, Mahamund M, Fuertes AB, Parra JB, Pajares JA, Bansal RC: Preparation of active carbons from coal part I. Oxidation of coal. *Fuel Processing Technology* 1996;47:19-38.
- [28] Laurendeal N.M. Heterogeneous kinetics of coal char gasification and combustion. *Progress in Energy and Combustion Science* 1978;4:221-70.
- [29] Jenkins SP, Nandi SP, Walker Jr PL. Reactivity of heat-treated coals in air at 500 °C. *Fuel* 1973;52:288-93.
- [30] Walker Jr PL. *Advances in coal utilization technology*. Chicago: Institute of Gas Technology; 1979.
- [31] Johnson JL. *Kinetics of coal gasification*. New York: Wiley; 1980.
- [32] Blake JH, Bopp GR, Jones JF, Miller MG, Tambo W. Aspects of the reactivity of porous carbons with carbon dioxide. *Fuel* 1967;46:115-25.
- [33] Allam R, White V, Ivens N, Simmonds M. The oxyfuel baseline: revamping heaters and boilers to oxyfiring by cryogenic air separation and flue gas recycle. In: Thomas DC, Benson

SM, editors. Carbon Dioxide Capture for Storage in Deep Geologic Formations – Results from the CO₂ Capture Project, Oxford, UK: Elsevier; 2005; vol. 1, chapter 26.

Tables

Table 1. Properties of the Cu60MgAl oxygen carrier particles.

Table 2. Properties of fresh and pre-treated “El Cerrejón” coal and the char prepared.

Table 3. Maximum value of the oxygen generation rate, $r_{O_2,red,max}$, for the Cu60MgAl material and calculated solids inventory in the fuel reactor for coal combustion, m_{FR} , as a function of the temperature.

Table 1. Properties of the Cu60MgAl oxygen carrier particles.

CuO content (wt.%)	60
Oxygen transport capability, R_{OC} (wt.%)	6.0
Crushing strength (N)	2.4
Density of particles (kg/m^3)	3860
XRD main phases	CuO, MgAl_2O_4

Table 2. Properties of fresh and pre-treated “El Cerrejón” coal and the char prepared.

	Fresh Colombian coal	Pre-treated Colombian coal	Char coal
C	70.8 %	65.8 %	79.8 %
H	3.9 %	3.3 %	0.7 %
N	1.7 %	1.6 %	1.3 %
S	0.5 %	0.6 %	0.6 %
O ⁽¹⁾	7.0	17.6	0.8
Moisture	7.5 %	2.3 %	6.4 %
Volatile matter	34.0 %	33.0 %	3.0 %
Fixed carbon	49.9 %	55.9 %	80.2 %
Ash	8.6 %	8.8 %	10.4 %

⁽¹⁾Oxygen to balance

Table 3. Maximum value of the oxygen generation rate, $r_{O_2,max}$, for the Cu60MgAl material and calculated solids inventory in the fuel reactor for coal combustion, m_{FR} , as a function of the temperature.

T_0 (°C)	T_{max} (°C)	$r_{O_2,max} \cdot 10^3$ (kgO ₂ /s per kg OC)	m_{FR} (kg OC/MW _{th})
900	930	2.1	39
925	955	2.6	32
950	980	2.8	29

Captions of figures

Fig. 1. Schematic design of the CLOU system using copper oxide as oxygen carrier.

Fig. 2. Equilibrium oxygen concentration over the CuO/Cu₂O system as a function of temperature.

Fig. 3. Schematic layout of the laboratory setup.

Fig. 4. Concentration of O₂, CO₂, CO, H₂ and CH₄ during a typical reduction and oxidation cycle with Cu60MgAl. The variation in the oxygen carrier conversion, X_{θ} , and temperature during the reduction and oxidation periods also is shown. $T_0 = 925$ °C; reduction in N₂ and oxidation with air; mass fraction of oxygen carrier: 100 wt.%; Coal batch: 2 g.

Fig. 5. Instantaneous oxygen generation rate, $r_{O_2,red}$, for the Cu60MgAl material as a function of the oxygen carrier to coal mass ratio. $T_0 = 925$ °C. Mass fraction of Cu60MgAl oxygen carrier in the reactor: 100 wt.%.

Fig. 6. (a) CO₂ yield and (b) ratio between the oxygen concentration at the reactor exit and at equilibrium conditions, $O_2/O_{2,eq}$, as a function of the oxygen carrier to coal mass ratio. $T_0 = 925$ °C. Mass fraction of Cu60MgAl oxygen carrier in the reactor: (□) 100 wt.%; (▲) 10 wt.%; (○) 2.5 wt.%.

Fig. 7. Instantaneous oxygen generation rate, $r_{O_2,red}$, for the Cu60MgAl oxygen carrier as a function of the oxygen carrier to coal mass ratio. $T_0 = 925$ °C. Mass fraction of Cu60MgAl oxygen carrier in the reactor: 10 wt.%.

Fig. 8. Instantaneous oxygen generation rate, $r_{O_2,red}$, for the Cu60MgAl oxygen carrier as a function of the oxygen carrier to coal mass ratio. $T_0 = 925$ °C. Mass fraction of Cu60MgAl oxygen carrier in the reactor: (□) 100 wt.%; (▲) 10 wt.%; (○) 2.5 wt.%.

Fig. 9. Instantaneous oxygen generation rate, $r_{O_2,red}$, for the Cu60MgAl oxygen carrier as a function of the oxygen carrier to coal mass ratio. $T_0 = 925$ °C. Mass fraction of Cu60MgAl oxygen carrier in the reactor: 2.5 wt.%. Fuel: (○) coal; (●) char.

Fig. 10. Char combustion rate, $(-r_{char})$, for the Cu60MgAl oxygen carrier as a function of the oxygen carrier to char mass ratio. $T_0 = 925$ °C. Mass fraction of Cu60MgAl oxygen carrier in the reactor: 2.5 wt.%.

Fig. 11. Calculated solids inventory in the fuel reactor for the Cu60MgAl oxygen carrier as a function of the oxygen carrier to coal mass ratio. $T_0 = 925$ °C. Mass fraction of Cu60MgAl oxygen carrier in the reactor: (□) 100 wt.%; (▲) 10 wt.%; (○) 2.5 wt.%.

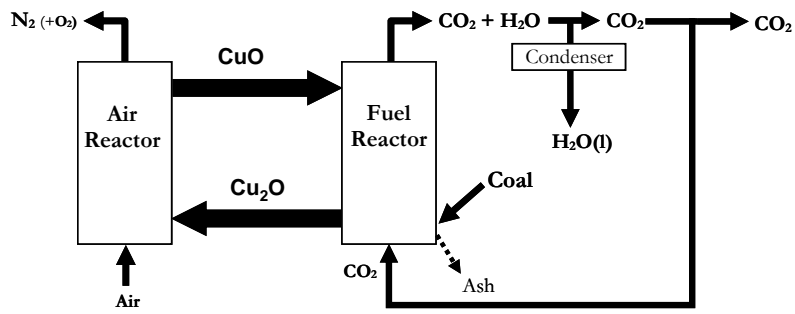


Fig. 1. Schematic design of the CLOU system using copper oxide as oxygen carrier.

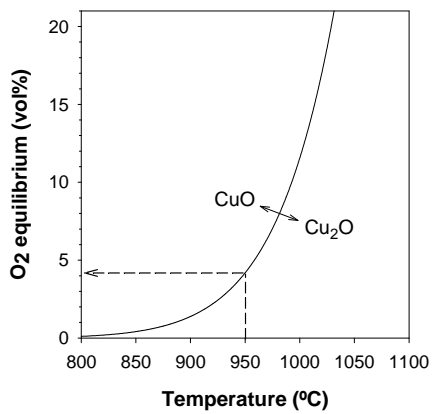


Figure 2. Equilibrium oxygen concentration over the CuO/Cu₂O system as a function of temperature.

|

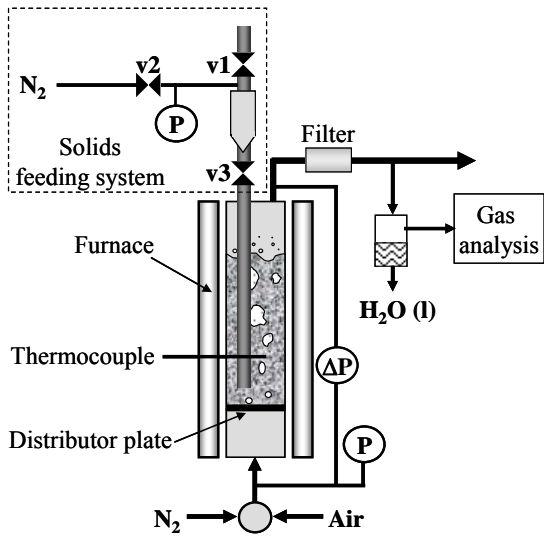


Fig. 3. Schematic layout of the laboratory setup.

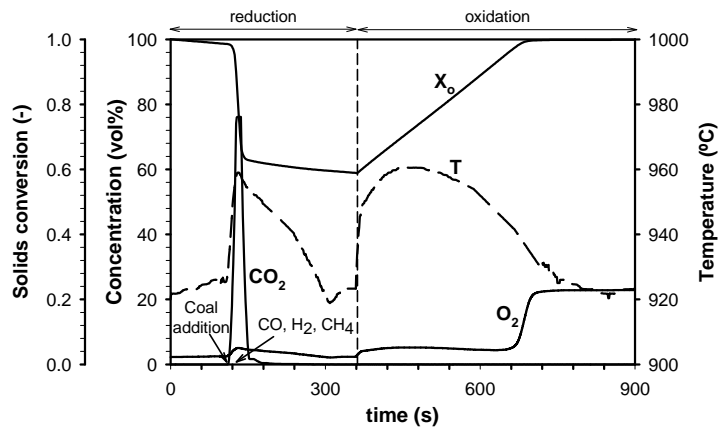


Fig. 4. Concentration of O_2 , CO_2 , CO , H_2 and CH_4 during a typical reduction and oxidation cycle with $Cu_{60}Mg_{40}$. The variation in the oxygen carrier conversion, X_o , and temperature during the reduction and oxidation periods also is shown. $T_0 = 925$ °C; reduction in N_2 and oxidation with air; mass fraction of oxygen carrier: 100 wt.%; Coal batch: 2 g.

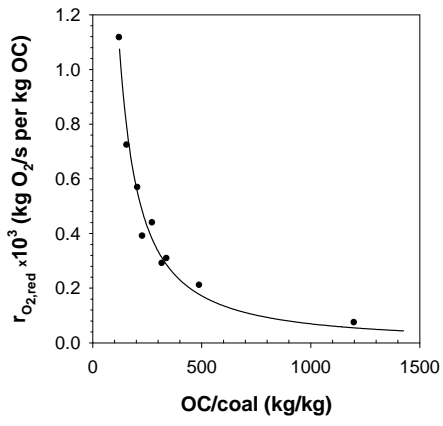


Fig. 5. Instantaneous oxygen generation rate, $r_{O_2,red}$, for the Cu60MgAl material as a function of the oxygen carrier to coal mass ratio. $T_0 = 925$ °C. Mass fraction of Cu60MgAl oxygen carrier in the reactor: 100 wt.%.

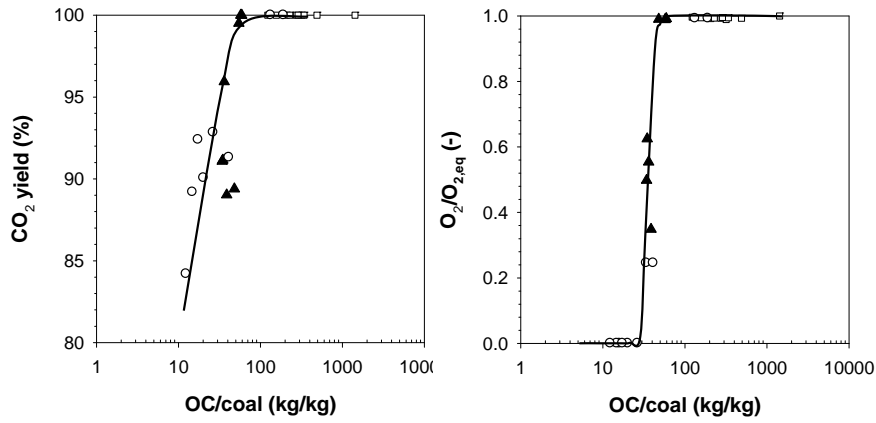


Fig. 6. (a) CO₂ yield and (b) ratio between the oxygen concentration at the reactor exit and at equilibrium conditions, $O_2/O_{2,eq}$, as a function of the oxygen carrier to coal mass ratio. $T_0 = 925$ °C. Mass fraction of Cu60MgAl oxygen carrier in the reactor: (□) 100 wt.%; (▲) 10 wt.%; (○) 2.5 wt.%.

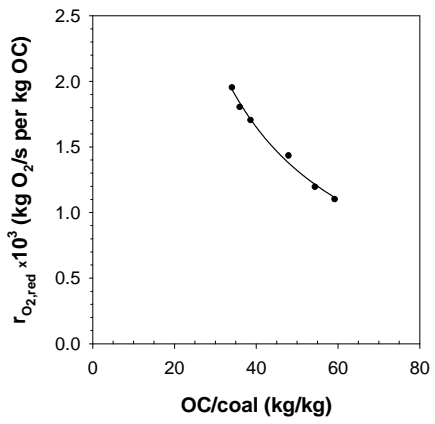


Fig. 7. Instantaneous oxygen generation rate, $r_{O_2,red}$, for the Cu60MgAl oxygen carrier as a function of the oxygen carrier to coal mass ratio. $T_0 = 925$ °C. Mass fraction of Cu60MgAl oxygen carrier in the reactor: 10 wt.%.

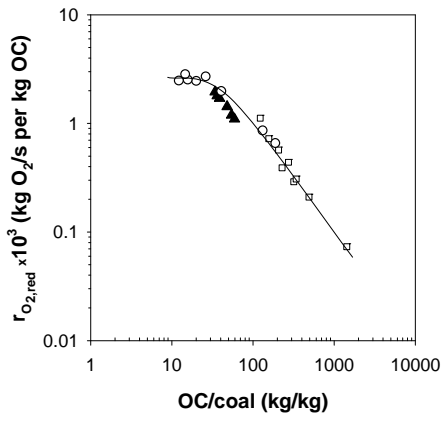


Fig. 8. Instantaneous oxygen generation rate, $r_{O_2,red}$, for the Cu60MgAl oxygen carrier as a function of the oxygen carrier to coal mass ratio. $T_0 = 925$ °C. Mass fraction of Cu60MgAl oxygen carrier in the reactor: (□) 100 wt.%; (▲) 10 wt.%; (○) 2.5 wt.%.

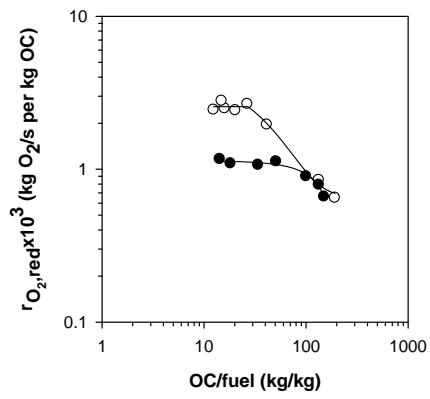


Fig. 9. Instantaneous oxygen generation rate, $r_{O_2, req}$, for the Cu60MgAl oxygen carrier as a function of the oxygen carrier to coal mass ratio. $T_0 = 925$ °C. Mass fraction of Cu60MgAl oxygen carrier in the reactor: 2.5 wt.%. Fuel: (○) coal; (●) char.

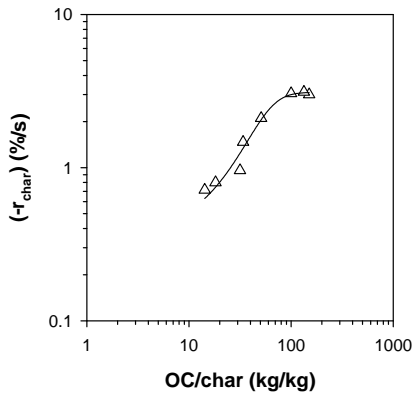


Fig. 10. Char combustion rate, $(-r_{char})$, for the Cu60MgAl oxygen carrier as a function of the oxygen carrier to char mass ratio. $T_0 = 925$ °C. Mass fraction of Cu60MgAl oxygen carrier in the reactor: 2.5 wt.%.

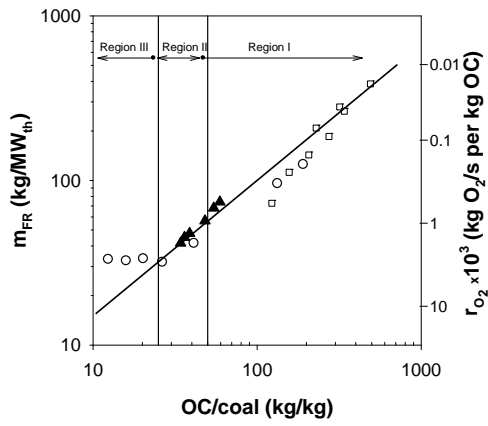


Fig. 11. Calculated solids inventory in the fuel reactor for the Cu60MgAl oxygen carrier as a function of the oxygen carrier to coal mass ratio. $T_0 = 925$ °C. Mass fraction of Cu60MgAl oxygen carrier in the reactor: (□) 100 wt.%; (▲) 10 wt.%; (○) 2.5 wt.%.